*Progress In Electromagnetics Research C, Vol. 132, 217–229, 2023*

# Triple Band Dual Sense Circularly Polarized Slot Antenna for S and C Band Applications

**Hirak K. Behera[1], Manas Midya[2], and Laxmi P. Mishra[1, *]**

**Abstract**—This paper proposes a microstrip-fed simple square slot patch antenna, which produces a triple band and is circularly polarized. The designed antenna consists of an L-shaped patch radiator in which the lower part of L is modified to a circle instead of a rectangle, and two rectangular strips are inserted from the opposite corners of the ground plane. Two small rectangular slits have also been used in the design to generate the triple band and widen the bandwidth too. The antenna has been fabricated and measured, and it shows a good agreement between them. The measured impedance bandwidths (IBWs) are 44.06% (2.3–3.6 GHz) and 73.68% (4.8–10.4 GHz), and the axial ratio bandwidths (ARBWs) are 37.29% (2.4–3.5 GHz), 13.6% (4.8–5.5 GHz), and 32.35% (5.7–7.9 GHz) in the lower, middle, and upper band, respectively.

## 1. INTRODUCTION

Different types of multiband antennas have been developed as a result of the spike in demand for devices that operate at numerous frequencies. Slot antennas have gained popularity among these because of their many benefits, including their low profile, simplicity in fabrication and mounting, and broad operating spectrum. Numerous multiband slot antenna designs exist due to these characteristics [1]. Circularly Polarized (CP) antennas and terminals offer an added benefit for mobile wireless devices because CP signals have superior propagation characteristics in multipath situations than linearly polarized ones. The majority of traditional techniques for creating CP slot antennas include adding strips, stubs, or cutting slits through the ground plane [2]. In [3] and [4] annular slot antenna structures are presented which generate dual bands and triple bands, respectively. In [4], the proposed antenna is designed using an L-shaped feed and two nonconcentric annular slot configurations, but the triple bands generated have low axial ratio bandwidth. In [5], the antenna consists of two layers: an electromagnetically coupled low-band patch present in the bottom layer and a probe-fed dual-band patch on the top layer. In [6], in order to achieve CP, a T-shaped slit is cut in the ground plane, and a rectangular parasitic stub is added to the antenna radiator. In [7], a slot antenna loaded with metallic strips, and a split-ring resonator (SRR) is proposed in which the CP bands are generated when the SRR and copper strips are excited by the microstrip feed. The coplanar waveguide (CPW)-fed antenna structure is proposed in [8] and [9]. In [8], a rectangular patch with two unequal rectangular strips is connected by a CPW feedline, and an inverted L-shaped stub is placed in the ground plane to create CP modes. In [10], an antenna is designed in which a U-shaped radiator, rotated by 45°, is placed at the top in which an I-shaped strip is connected, and then an inverted L-shaped strip is connected to the end of the I-shaped strip in order to generate different CP modes. In [11], the antenna is designed by using a hexagonal slot with L-shaped slits. Three slits are added to the hexagonal slots for generating CP modes at different frequencies. [12] presents a structure in which circular polarization is achieved by

*Received 21 February 2023, Accepted 18 April 2023, Scheduled 2 May 2023*

* Corresponding author: Laxmi Prasad Mishra (laxmimishra@soa.ac.in).

[1] Department of ECE, S 'O' A (Deemed to be University), Bhubaneswar, Odisha, India. [2] Department of ECE, Institute of Engineering & Management, Kolkata, India.

placing a semi-circular radiating patch along a slit in it and a modified structure in the ground plane. Similar to [7], Ref. [13] has a compact antenna structure that is loaded with a D-shaped complementary split ring resonator (SRR) which shows dual-band polarization. Likewise, in [14], a printed inverted F antenna loaded with a rectangular complementary split ring resonator (CSSR) is designed and studied based on the various antenna parameters. A dual-band dual-sense CP antenna consisting of U- and L-shaped patches is designed for the implementation purpose in WLAN and WiMax application areas [15]. Similarly, in [16], a U-shaped patch is considered along which an L-shaped parasitic patch is also used which results in the generation of a dual-band CP antenna.

To overcome those complexities, a simple square slot antenna is designed and fabricated in which an L-shaped radiator is placed in which instead of a rectangle a circle is introduced in the lower part of the radiator, and the prototype is modified which is referred from [17]. The simulated results show that it achieves an Impedance Bandwidth (IBW) of 2.4–3.5 GHz (37.29%) and then 5–10 GHz (66.66%) in the lower and upper bands, respectively, whereas the axial ratio falls under the 3 dB range of 2.5–3.5 GHz (33.33%), 5–5.5 GHz (9.52%), and 5.7–7.6 GHz (28.57%) in the lower, middle, and upper bands, respectively. Considering the resonating frequency to be 3 GHz, some articles are compared with the proposed structure regarding their antenna size, IBWs, and Axial Ratio Bandwidths (ARBWs) which are listed in Table 1. The antenna parameters are calculated using some prefixed design equations which are listed below [18].

The expression of $\varepsilon_{reff}$ is given by:

$$\varepsilon_{reff} = \frac{\varepsilon_r + 1}{2} + \frac{\varepsilon_r - 1}{2}\left[1 + 12\frac{h}{W}\right]^{\frac{-1}{2}} \tag{1}$$

**Table 1.** Comparison with existing antennas.

| Reference | Size ($\lambda^3$) | Lower IBW (%, GHz) | Middle IBW (%, GHz) | Upper IBW (%, GHz) | Lower ARBW (%, GHz) | Middle ARBW (%, GHz) | Upper ARBW (%, GHz) |
|---|---|---|---|---|---|---|---|
| [4] | $0.95\lambda_0 \times 0.93\lambda_0$ $\times 0.00813\lambda_0$ | 9%, 1.16–1.27 | 2.5%, 1.55–1.59 | 27%, 2–2.62 | 7.28%, 1.190-1.28 | 1.26%, 1.57–1.59 | 5.56%, 2.45–2.59 |
| [5] | $0.4\lambda_0 \times 0.4\lambda_0$ $\times 0.03\lambda_0$ | 4.08%, 2.4–2.5 | 3.4%, 3.46–3.58 | 7.35%, 5.63–6.06 | 0.4%, 2.48–2.49 | 1.12%, 3.54–3.58 | 0.7%, 5.7–5.74 |
| [6] | $0.27\lambda_0 \times 0.27\lambda_0$ $\times 0.01\lambda_0$ | 116.77%, 3.1–11.8 | | | 3.78%, 3.63–3.77 | 4.54%, 4.95–5.18 | 4.3%, 9.55–9.97 |
| [7] | $0.5\lambda_0 \times 0.5\lambda_0$ $\times 0.0156\lambda_0$ | 21.4%, 1.48–1.87 | 12.8%, 2.39–2.71 | 4.5%, 3.02–3.16 | 4.37%, 1.77–1.85 | 11.9%, 2.4–2.7 | 3.57%, 3.04–3.15 |
| [8] | $0.5\lambda_0 \times 0.5\lambda_0$ $\times 0.0158\lambda_0$ | 91.84%, 2.72–7.34 | | | 13.55%, 3.3–3.78 | 8.17%, 5.4–5.86 | |
| [9] | $0.63\lambda_0 \times 0.75\lambda_0$ $\times 0.016\lambda_0$ | 71.63%, 1.81–3.83 | | | 27.45%, 2.2–2.9 | 7.1%, 3.4–3.65 | |
| [10] | $0.5\lambda_0 \times 0.52\lambda_0$ $\times 0.0152\lambda_0$ | 21.35%, 2.35–2.8 | 76.63%, 3.3–7.4 | | 12%, 2.35–2.65 | 10%, 3.3–3.65 | 4.4%, 5.6–5.85 |
| [11] | $0.6\lambda_0 \times 0.6\lambda_0$ $\times 0.0152\lambda_0$ | 33.16%, 3.22–4.5 | 22.72%, 4.76–5.98 | | 1.7%, 3.49–3.55 | 3.86%, 4.06–4.22 | 5.23%, 5.03–5.3 |
| Proposed antenna | $0.6\lambda_0 \times 0.6\lambda_0$ $\times 0.01\lambda_0$ | 44.06%, 2.3–3.6 | 73.68%, 4.8–10.4 | | 37.29%, 2.4–3.5 | 13.6%, 4.8–5.5 | 32.35%, 5.7–7.9 |

The change in length is given by:

$$\frac{\Delta L}{h} = 0.412 \frac{(\varepsilon_{reff} + 0.3)\left(\frac{W}{h} + 0.264\right)}{(\varepsilon_{reff} - 0.258)\left(\frac{W}{h} + 0.8\right)} \tag{2}$$

The effective length ($L_{eff}$) becomes:

$$L_{eff} = L + 2\Delta L \tag{3}$$

The effective length, for a resonance frequency ($f_0$), is given by:

$$L_{eff} = \frac{C}{2f_0\sqrt{\varepsilon_{reff}}} \tag{4}$$

Width ($W$) is given by:

$$W = \frac{C}{2f_0\sqrt{\frac{(\varepsilon_r + 1)}{2}}} \tag{5}$$

## 2. ANTENNA DESIGN AND GEOMETRY

The structural shape of the proposed antenna is shown in Figure 1. The overall area covered by the proposed antenna is $60 \times 60\,\text{mm}^2$. A $50\,\Omega$ microstrip feed line is used to design the antenna which is further fabricated on an FR4 substrate having a thickness of 1 mm and relative permittivity of 4.4. A modified L-shaped radiator is printed on the upper side of the substrate, whose work is to generate the resonance frequency bands whereas a modified ground plane structure is placed on the bottom side of the substrate. The patch consists of a rectangle ($S5 \times S6$), and the lower part of the rectangle is merged with a circular stub of radius 3.3 mm and is fed by a microstrip feed line. Two rectangular strips ($S1 \times S2$ and $S3 \times S4$) are placed in the opposite corners of the structure in the ground plane to generate CP waves. Two rectangular slits are also present in the structure. One slit ($a \times b$) is cut in the rectangular strip $S3 \times S4$, and the second slit ($c \times d$) is cut in the rectangular strip $S1 \times S2$ to generate the triple band as well as widen the bandwidth. The proposed antenna is compact in size, and its overall dimension is $60 \times 60 \times 1\,\text{mm}^3$ which is simulated with the help of Ansys HFSS and is also fabricated and measured. The desired parametric values are mentioned in Table 2.

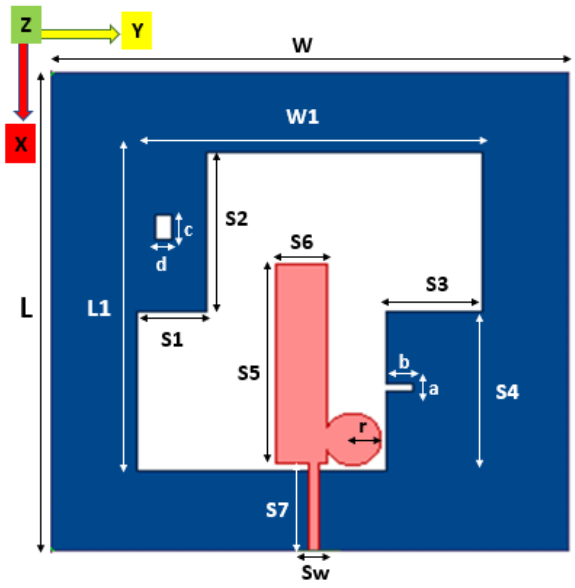


**Figure 1.** Proposed antenna.

**Table 2.** Parametric values of the designed antenna.

| Parameters | Dimension (mm) | Parameters | Dimension (mm) |
|---|---|---|---|
| $L$ | 60 | $W$ | 60 |
| $L1$ | 40 | $W1$ | 40 |
| $S1$ | 8 | $S2$ | 20 |
| $S3$ | 11 | $S4$ | 20 |
| $S5$ | 25 | $S6$ | 6 |
| $S7$ | 11 | $Sw$ | 1 |
| $a$ | 1 | $b$ | 3 |
| $c$ | 3 | $d$ | 2 |
| $r$ | 3.3 | | |

## 3. DESIGN PROCEDURE

The evolution process of the designed antenna is explained in a step-by-step process and is shown in Figure 2. The antenna is said to be in good working condition and follows the CP mechanism when the axial ratio falls under the range of impedance bandwidth. Here five antennas are shown in which Ant 1, Ant 2, Ant 3, and Ant 4 are the different stages towards the realization of the CP antenna, and Ant 5 is

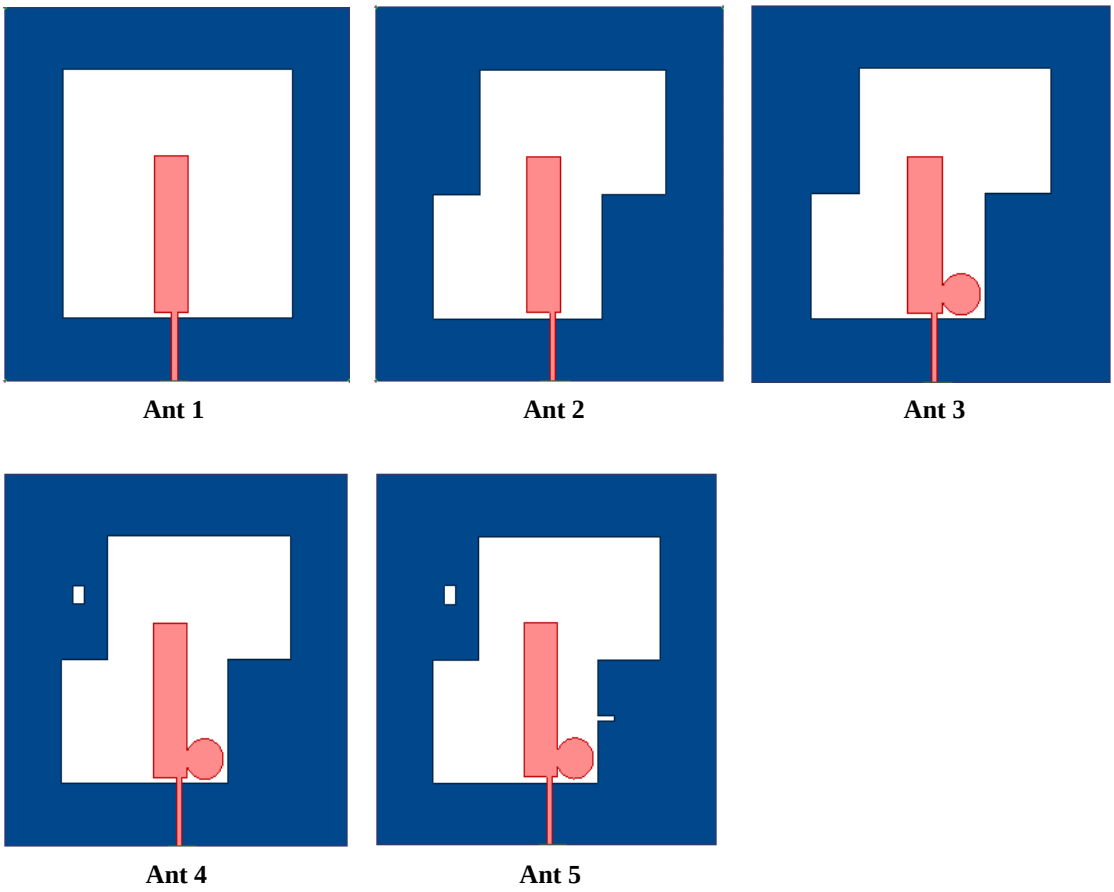


**Figure 2.** Steps for realizing the proposed antenna.

the final proposed antenna. Ant 1 is a simple structure having a square slot cut in the ground plane of the desired value mentioned in Table 2 and is fed by a microstrip feed line having a rectangular patch. In Ant 2, the microstrip feedline is shifted toward the right side of the patch, and the two rectangular strips $S1 \times S2$ and $S3 \times S4$ are placed in the opposite corners of the ground plane. In Ant 3, a circle of radius 3.3 mm is placed in the lower end of the patch to give it an L shape in which instead of a rectangle, a circle is placed. In Ant 4, a small slit of size $3 \times 2$ is placed on the rectangle $S1 \times S2$. Ant 5 is the final proposed antenna in which again a small strip of size $1 \times 3$ is placed on the rectangle $S3 \times S4$.

## 4. RESULTS AND DISCUSSION

The simulated software work is carried out with the help of Ansys HFSS ver. 21. To understand the design procedure, the antenna evolution steps are clearly shown in Figure 2 and explained in the design procedure section. To visualize the performance of the desired antenna, the impedance bandwidth and axial ratio values of Ant 1–5 are plotted and shown in Figure 3. Figure 3(a) shows the Impedance bandwidth Vs Frequency plot, and Figure 3(b) shows the Axial ratio Vs Frequency plot. From both plots, we can observe that Ant 1 is linearly polarized as the axial ratio does not fall under the 3 dB range, and the impedance bandwidth ranges from 6.2–7.6 GHz. In Ant 2, the feedline is shifted towards the right side, and then two square slots of asymmetric size are placed in the opposite corners of the ground plane. Here the antenna is also linearly polarized as it does not fall under the 3 dB range, and its impedance bandwidth lies from 6.3 to 7.4 GHz. Ant 3 comes up with a structure having a circle placed in the lower end of the rectangular patch. Its impedance bandwidth lies from 2.5 to 3.5 GHz, and again it falls from 5.1 to 10 GHz. The axial ratio of Ant 3 lies under the impedance bandwidth range, and it goes from 2.6 to 3.5 GHz and again from 6.3 to 6.7 GHz which shows that the antenna is circularly polarized. In Ant 4, a small slit is cut in the $S1 \times S2$ rectangle which shows that the impedance bandwidth ranges from 2.5 to 3.5 GHz and again from 5.1 to 10.1 GHz while its axial ratio also falls in this range which lies from 2.6 to 3.4 GHz and again from 6.1 to 6.7 GHz. Finally, Ant 5 is the proposed antenna in which again a small slit is cut in the $S3 \times S4$ rectangle from which we can see that the impedance bandwidth goes from 2.4 to 3.5 GHz and again from 5 to 10 GHz, and the axial ratio bandwidth also falls in the impedance bandwidth range which lies in 2.5–3.5 GHz, 5–5.5 GHz, and 5.7–7.6 GHz. Hence as the axial ratio falls under the impedance bandwidth range, we can clearly state that our designed antenna is circularly polarized.

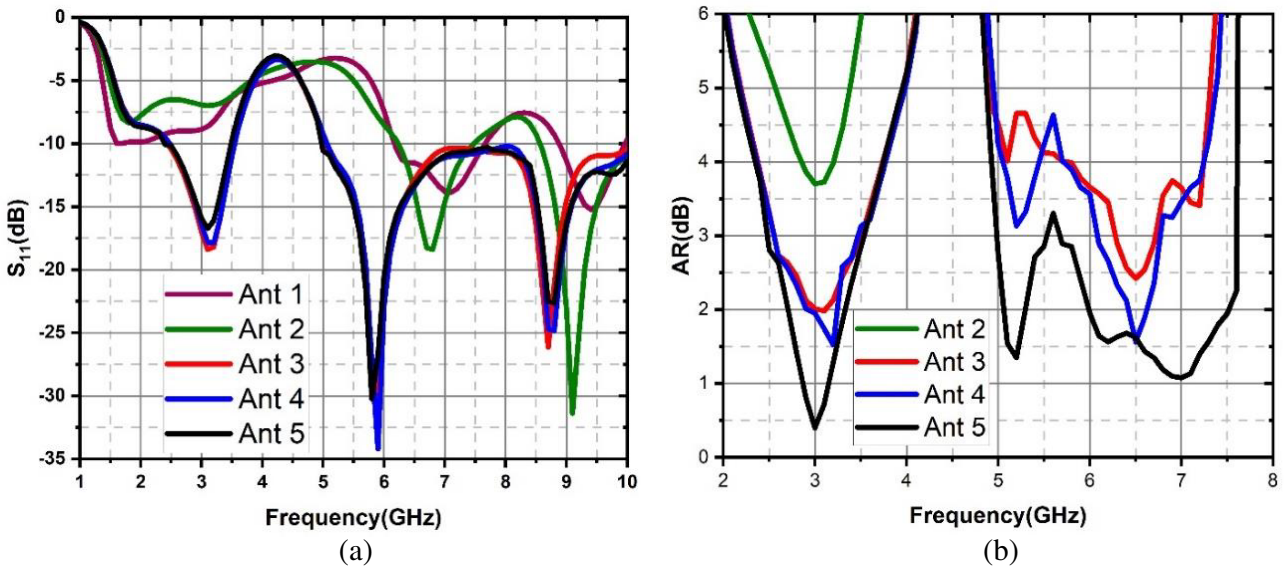


**Figure 3.** Simulated (a) $S_{11}$, (b) AR of Ant 1–5.

## 5. PARAMETRIC ANALYSIS

The proposed antenna achieves circular polarization when two rectangular strips of different sizes are introduced in the ground plane along with placing a circular stub in the patch. Results have also been observed by changing the slot width and varying the size of two slits. Here six parameters, rectangle $S1 \times S2$, rectangle $S3 \times S4$, circle radius ($r$), slot width ($Sw$), and two slits ($a \times b$) and ($c \times d$) are considered for the parametric analysis and have been analyzed with the help of Ansys HFSS by varying one parameter at one time while keeping the other parameters constant.

### 5.1. Effects due to Rectangle $S1$ and $S2$

Figure 4 shows the plot of impedance bandwidth and axial ratio in terms of varying the $S1$ and $S2$ for different values. Here four values of $S1$ and $S2$ are considered among which $S1 = 8\,\text{mm}$ and $S2 = 20\,\text{mm}$ are taken into account. From Figure 4(a) we can see that the $S_{11}$ parameters are almost the same for all 4 values of $S1$ and $S2$, but the difference can be noticed in the axial ratio graph for which rectangle $8 \times 20\,\text{mm}^2$ is considered for the design.

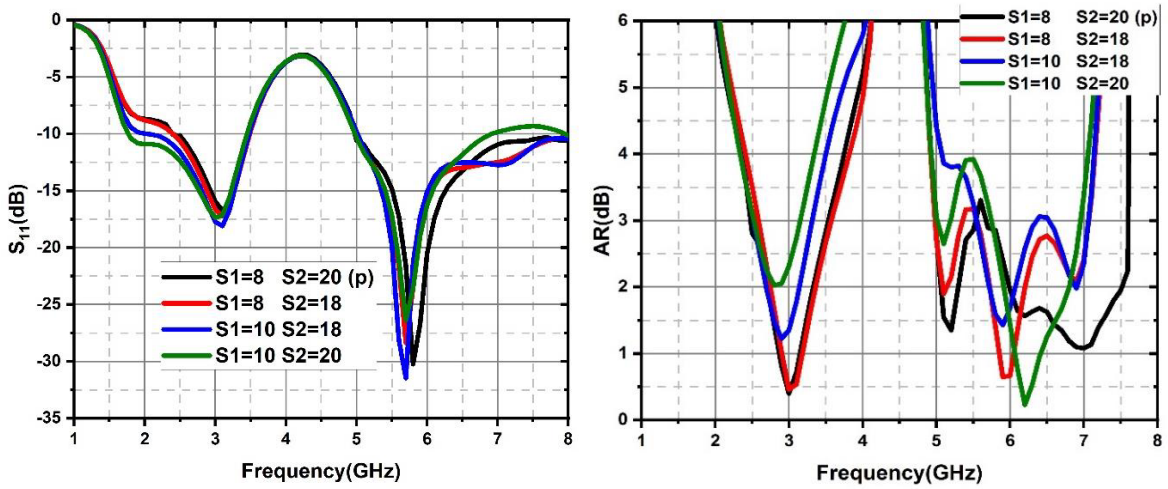


**Figure 4.** Effects of $S1$ and $S2$ on antenna performances (a) $S_{11}$, (b) axial ratio.

### 5.2. Effects due to Rectangle $S3$ and $S4$

In Figure 5, the effects of rectangle $S3 \times S4$ on the antenna have been studied. Here from Figure 5(a), we can observe that all four values of $S3$ and $S4$ give almost the same results, but a noticeable change is found in Figure 5(b) which shows the axial ratio graph. By considering both plots, we find that $S3 = 11\,\text{mm}$ and $S4 = 20\,\text{mm}$ give better result than other values.

### 5.3. Effects by Circular Stub Radius ($r$)

Figure 6 shows the effect on the antenna due to the variation of the circle's radius. Here 3 values of radius $r = 3.2$, 3.3, and 3.4 mm are taken into account among which 3.3 mm is chosen for the design as it shows good results both in terms of impedance and axial bandwidth.

### 5.4. Effects in the Variation of Slot Width ($Sw$)

In Figure 7, the variation of slot width in terms of antenna design is shown. Here 3 values of $Sw$ that are 0.5, 1, and 1.5 mm are taken for the analysis purpose among which $Sw = 1\,\text{mm}$ shows the best

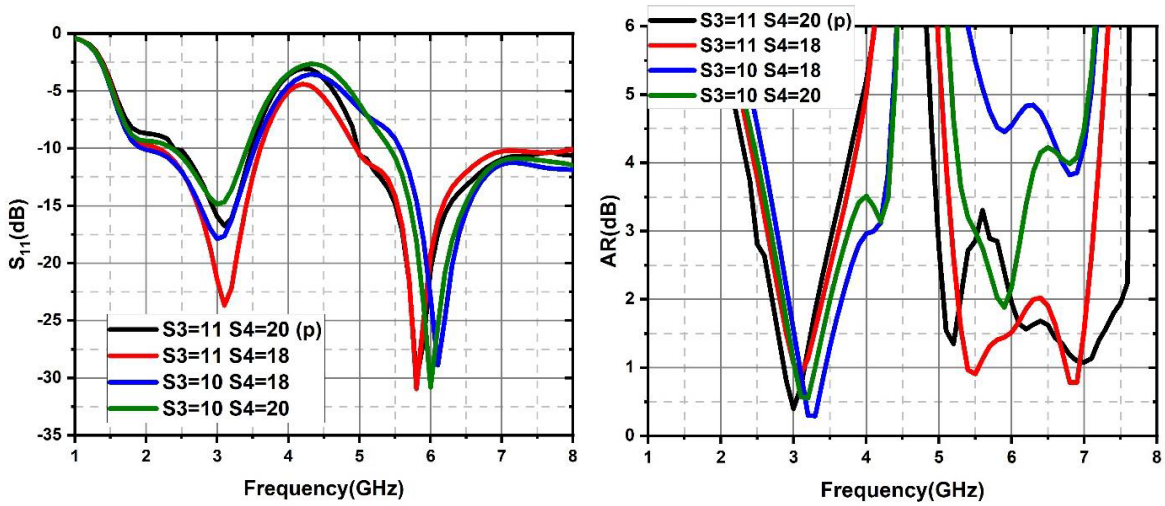


**Figure 5.** Effects of $S3$ and $S4$ on antenna performances (a) $S_{11}$, (b) axial ratio.

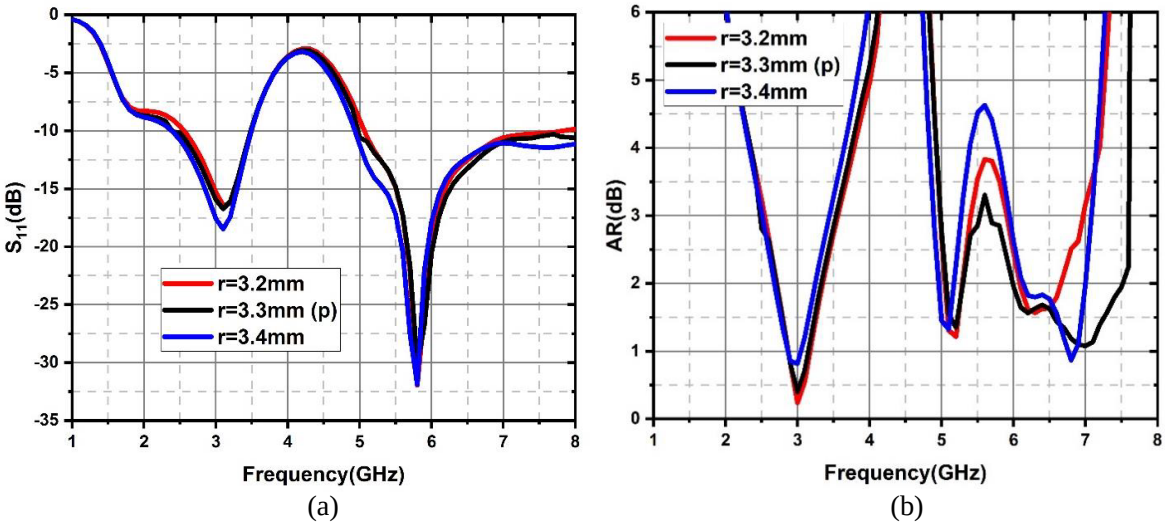


**Figure 6.** Effects of circle radius ($r$) on antenna performances (a) $S_{11}$, (b) axial ratio.

output both in terms of the $S_{11}$ parameter and axial ratio. So 1 mm width is chosen for the design as the parametric value for $Sw$.

### 5.5. Effects due to Slit $a$ and $b$

Figure 8 shows the effect of slit sizes $a$ and $b$ on antenna design. Here 3 values of $a$ and $b$ are considered among which $a = 1$ mm and $b = 3$ mm are considered. From Figure 8(a) we can observe that the $S_{11}$ parameters for all three values are same, but the $1 \times 3$ slit is chosen by only focusing on the axial ratio parameter which we can observe from Figure 8(b).

### 5.6. Effects due to Slit $c$ and $d$

Figure 9 shows the effect due to slits $c$ and $d$. Here also 3 values of $c$ and $d$ are taken for analysis, but $c = 3$ mm and $d = 2$ mm are considered for the design purpose as it gives a satisfactory result in

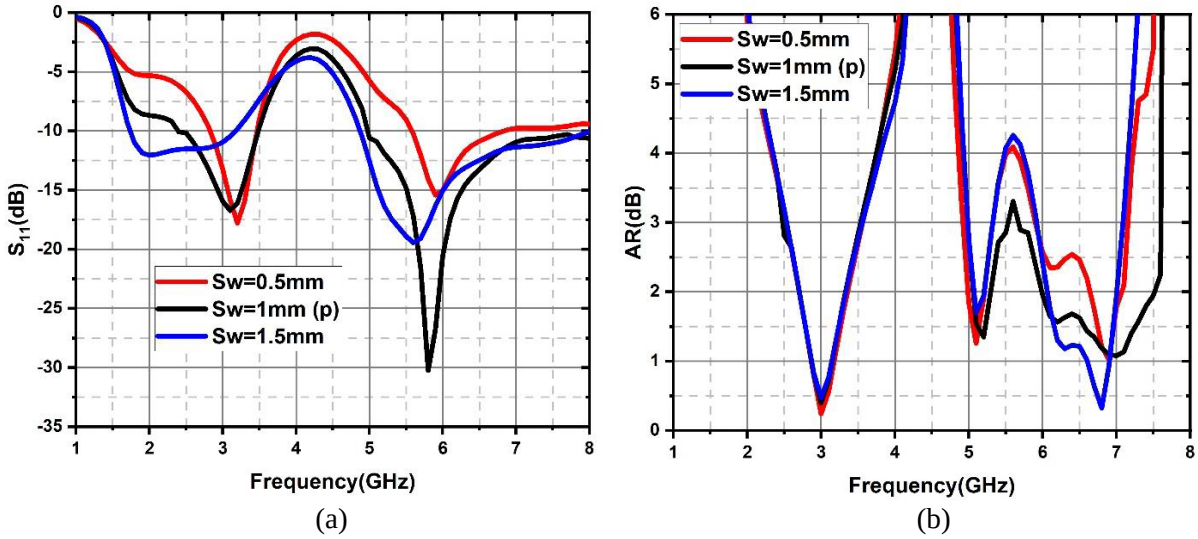


(a) (b)

**Figure 7.** Effects of $Sw$ on antenna performances (a) $S_{11}$, (b) axial ratio.

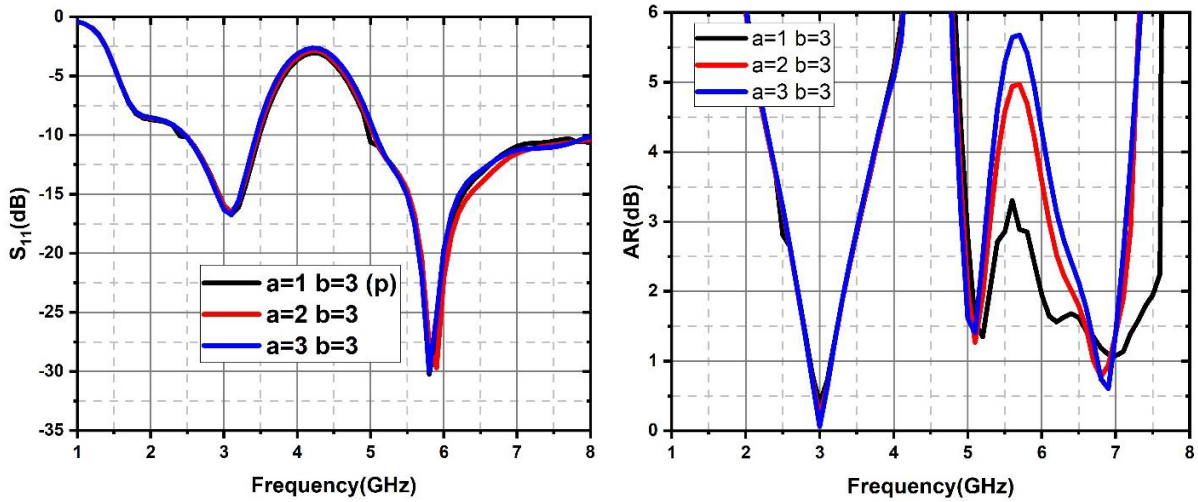


(a) (b)

**Figure 8.** Effects of $a$ and $b$ on antenna performances (a) $S_{11}$, (b) axial ratio.

comparison to the other two values both in terms of $S_{11}$ and axial ratio.

## 6. EXPERIMENTAL VERIFICATION

Figure 10 represents the plot of simulated and measured values of impedance bandwidths and axial ratio bandwidths of the designed antenna. From Figure 10(a) we can observe that the simulated impedance bandwidth covers 2.4–3.5 GHz in the lower band and 5–10 GHz in the upper band whereas the measured impedance bandwidth covers 2.3–3.6 GHz and 4.8–10.4 GHz in the lower and upper bands, respectively. Similarly, from Figure 10(b) we can say that the simulated AR lies in 2.5–3.5 GHz, 5–5.5 GHz, and 5.7–7.6 GHz in the lower band, middle band, and upper band, respectively, whereas the measured results show that the AR lies in 2.4–3.5 GHz, 4.8–5.5 GHz, and 5.7–7.9 GHz in lower, middle, and upper bands, respectively. We can observe that the simulated and measured values hold a good agreement between them.

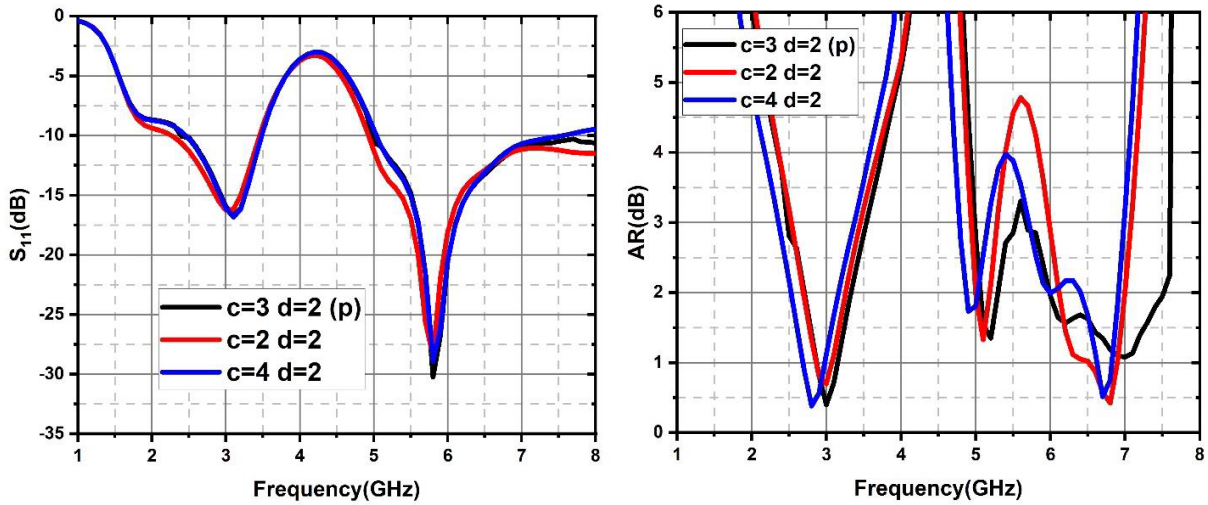


**Figure 9.** Effects of $c$ and $d$ on antenna performances (a) $S_{11}$, (b) axial ratio.

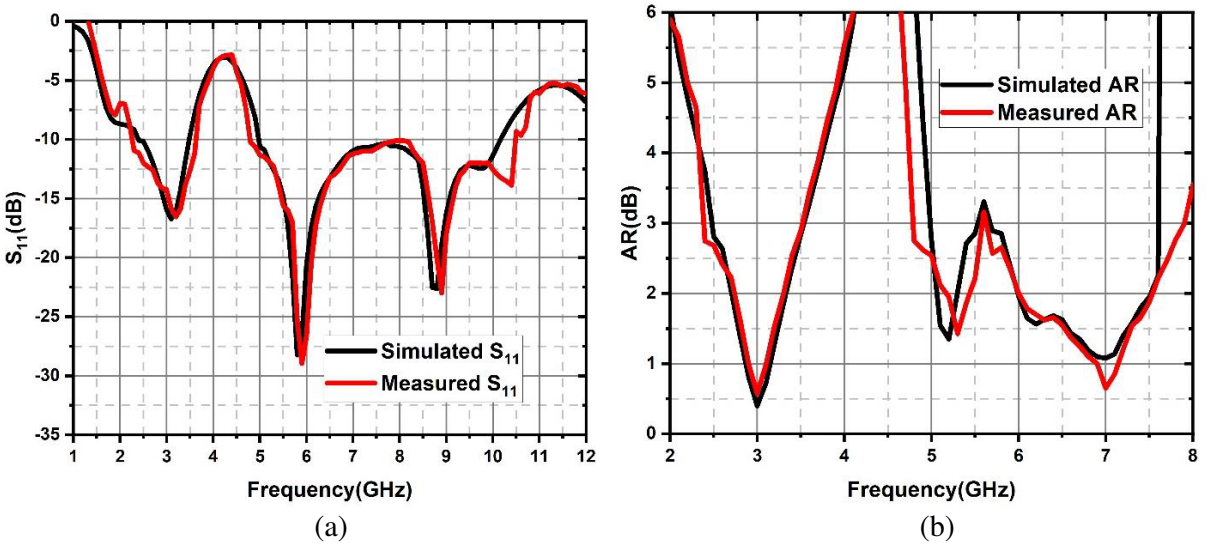


**Figure 10.** Simulated vs measured (a) $S_{11}$, (b) AR.

The radiation patterns of the proposed antenna are shown in Figure 11. For the three frequencies, 3 GHz, 5.2 GHz, and 6.5 GHz, both $XZ$ and $YZ$ planes are represented in which both simulated and measured values are noted in the graph, and it can be observed that they are very similar to each other. Further, it can be stated that the antenna is Right Hand Circularly Polarized (RHCP) in the lower band at 3 GHz frequency and Left Hand Circularly Polarized (LHCP) both at 5.2 GHz and 6.5 GHz in the middle and upper bands, respectively.

Figure 12 represents the graph of antenna gain for both the simulated and measured values whose frequency range varies from 2 GHz to 8 GHz as the axial ratio falls in between this range.

The proposed antenna is simulated using ANSYS HFSS software, and for its practical use, the antenna prototype is fabricated on an FR4 substrate and is measured inside an anechoic chamber. Figure 13 represents the top and bottom views of the fabricated structure.

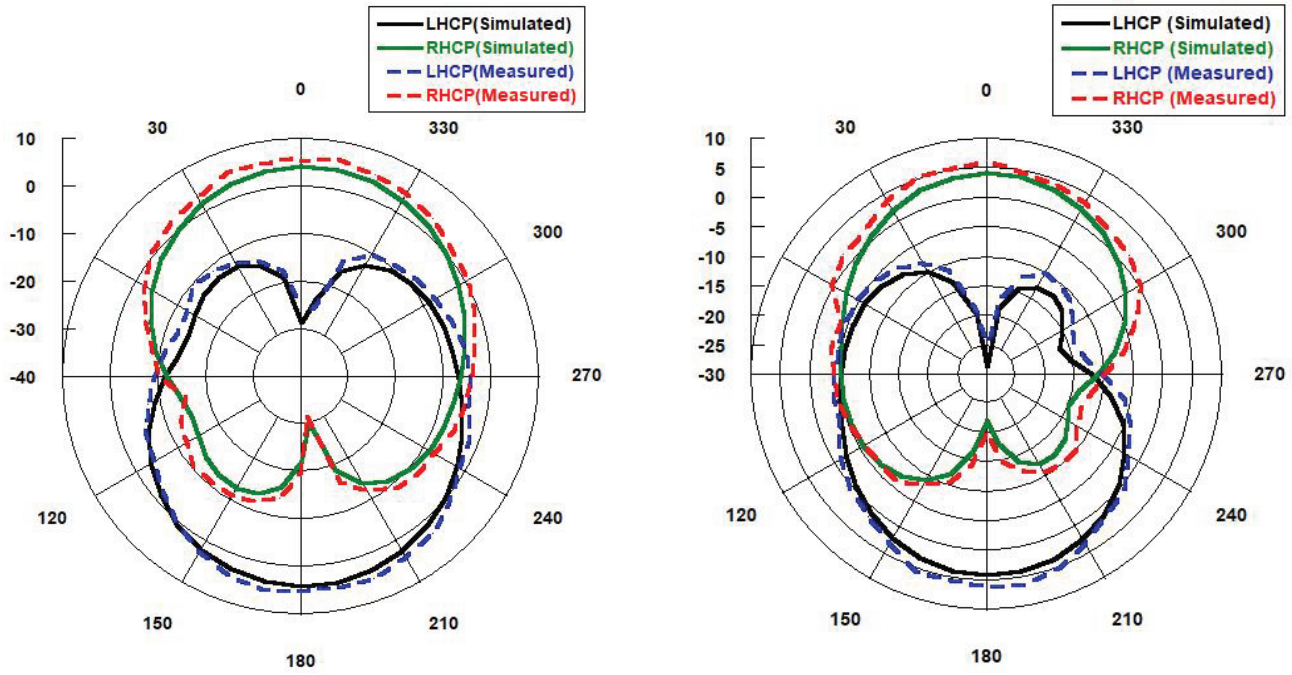
LHCP(Simulated)
RHCP(Simulated)
LHCP(Measured)
RHCP(Measured)
0
30
330
300
270
240
210
180
150
120
10
0
-10
-20
-30
-40
LHCP (Simulated)
RHCP (Simulated)
LHCP (Measured)
RHCP (Measured)
10
5
0
-5
-10
-15
-20
-25
-30

(a)

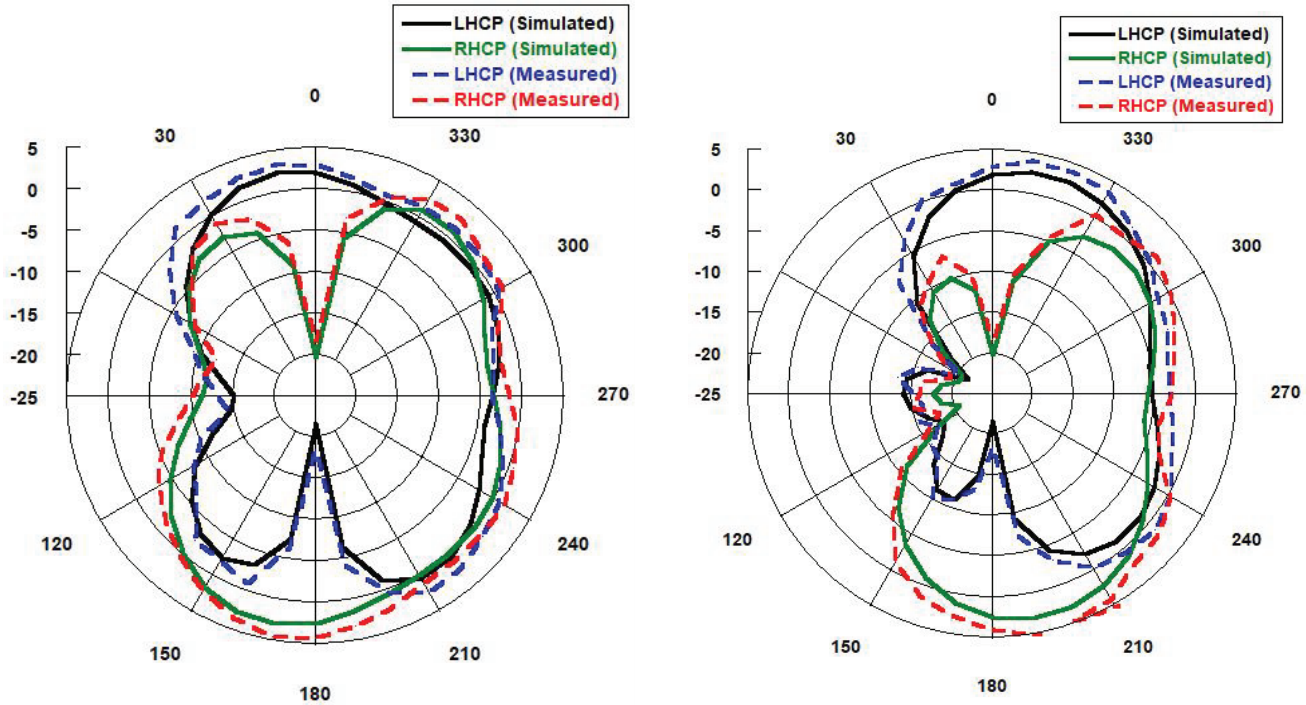
LHCP (Simulated)
RHCP (Simulated)
LHCP (Measured)
RHCP (Measured)
0
30
330
300
270
240
210
180
150
120
5
0
-5
-10
-15
-20
-25

(b)

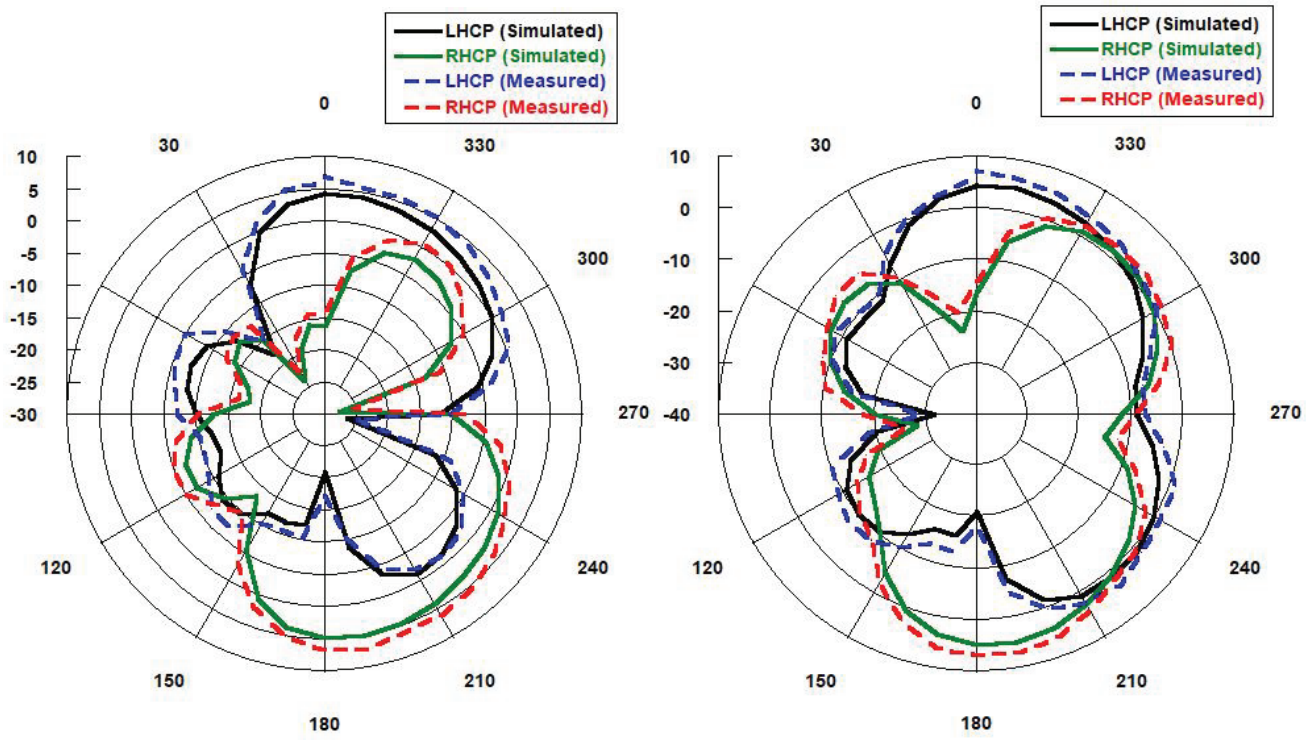


(c)

**Figure 11.** Simulated and measured radiation patterns at (a) 3 GHz, (b) 5.2 GHz, and (c) 6.5 GHz.

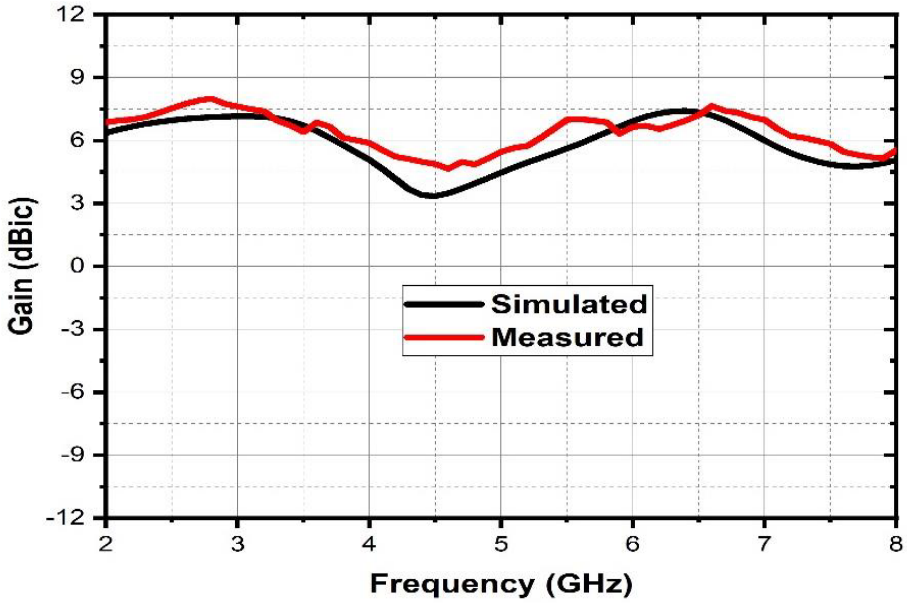


**Figure 12.** Simulated and measured gain of the designed antenna within the AR band.

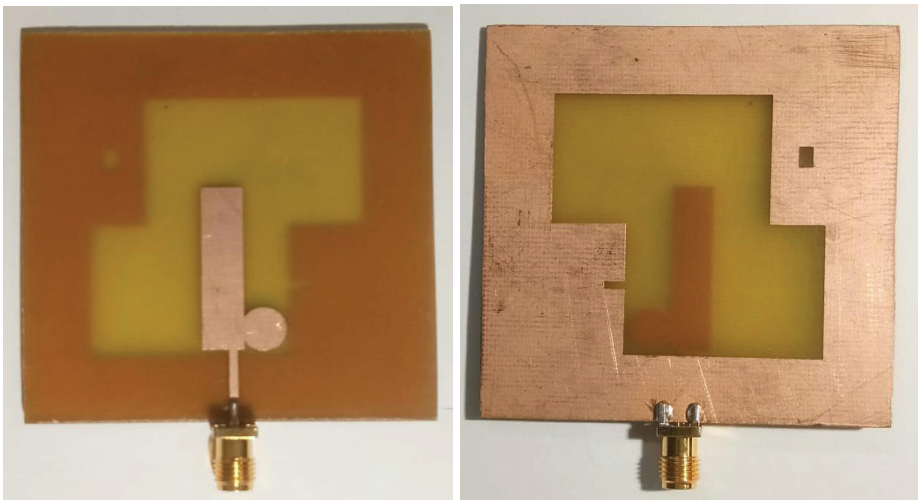

(a) (b)

**Figure 13.** Antenna prototype. (a) Top view. (b) Bottom view.

## 7. CONCLUSION

A triple band dual sense circularly polarized antenna is proposed. The antenna was simulated with the help of Ansys HFSS software and also fabricated and measured successfully. The measured data shows that it attains a 10 dB return loss from frequencies 2.3–3.6 GHz and 4.8–10.4 GHz in the lower and upper bands, respectively, whereas the axial ratio graph shows that it falls under the 3 dB range in 2.4–3.5 GHz, 4.8–5.5 GHz, and 5.7–7.9 GHz in the lower, middle, and upper bands, respectively, which indicates that the antenna is circularly polarized as it falls under the impedance bandwidth range. The antenna is RHCP in the lower frequency band whereas it is LHCP in the middle and upper-frequency bands. Simulated and measured results hold a good agreement between them. Finally, the designed antenna can be practically used in both S-band (2–4 GHz) and C-band (4–8 GHz) frequency ranges.

## REFERENCES

1. Gao, S., Q. Luo, and F. Zhu, *Circularly Polarized Antennas*, Wiley-IEEE Press, New York, NY, 2013.
2. Behera, H. K., M. Midya, and L. P. Mishra, "Performance enhancement of a compact circularly polarized slot antenna using corner truncation," *Progress In Electromagnetics Research C*, Vol. 126, 197–206, 2022.
3. Hsieh, W.-T., T.-H. Chang, and J.-F. Kiang, "Dual-band circularly polarized cavity-backed annular slot antenna for GPS receiver," *IEEE Transactions on Antennas and Propagation*, Vol. 60, No. 4, 2076–2080, Apr. 2012.
4. Wang, L., Y.-X. Guo, and W. X. Sheng, "Tri-band circularly polarized annular slot antenna for GPS and CNSS applications," *Journal of Electromagnetic Waves and Applications*, Vol. 26, Nos. 14–15, 1820–1827, Aug. 2012.
5. Bao, X. L. and M. J. Ammann, "Printed triple-band circularly polarised antenna for wireless systems," *Electronics Letters*, Vol. 50, No. 23, 1664–1665, 2014.
6. Li, G., H. Zhai, T. Li, L. Li, and C. Liang, "A compact ultra wideband antenna with triple-sense circular polarization," *2013 Proceedings of the International Symposium on Antennas & Propagation*, Vol. 1, 531–534, 2013.

7. Paul, P. M., K. Kandasamy, and M. S. Sharawi, "A triband circularly polarized strip and SRR-loaded slot antenna," *IEEE Transactions on Antennas and Propagation*, Vol. 66, No. 10, 5569–5573, Oct. 2018.
8. Midya, M., S. Bhattacharjee, and M. Mitra, "CPW-fed dual-band dual-sense circularly polarized antenna for WiMAX application," *Progress In Electromagnetics Research Letters*, Vol. 81, 113–120, 2019.
9. Saini, R. K., S. Dwari, and M. K. Mandal, "CPW-fed dual-band dual-sense circularly polarized monopole antenna," *IEEE Antennas and Wireless Propagation Letters*, Vol. 16, 2497–2500, 2017.
10. Park, H. and T. V. Hoang, "Very simple 2.45/3.5/5.8 GHz triple-band circularly polarised printed monopole antenna with bandwidth enhancement," *Electronics Letters*, Vol. 50, 1792–1793, 2014.
11. Baek, J. G. and K. C. Hwang, "Triple-band unidirectional circularly polarized hexagonal slot antenna with multiple L-shaped slits," *IEEE Transactions on Antennas and Propagation*, Vol. 61, No. 9, 4831–4835, Sept. 2013.
12. Midya, M., S. Bhattacharjee, and M. Mitra, "Triple-band dual-sense circularly polarised planar monopole antenna," *IET Microwaves, Antennas & Propagation*, Vol. 13, No. 12, 2020–2025, 2019.
13. Singh, G., B. K. Kanaujia, V. K. Pandey, D. Gangwar, and S. Kumar, "Design of compact dual-band patch antenna loaded with D-shaped complementary split ring resonator," *Journal of Electromagnetic Waves and Applications*, Vol. 16, No. 18, 1–16, 2019.
14. Chatterjee, A., M. Midya, L. P. Mishra, and M. Mitra, "Compact dual polarized branch-line printed inverted-F antenna covering both cellular and non-cellular bands with independent tuning," *Progress In Electromagnetics Research C*, Vol. 101, 95–104, 2020.
15. Bag, B., P. Biswas, R. Mondal, S. Biswas, and P. P. Sarkar, "Dual-band dual-sense circularly polarized U- and L-shaped strip monopole antenna for WiMAX/WLAN applications," *Journal of Electromagnetic Waves and Applications*, Vol. 16, No. 18, 1–15, 2019.
16. Midya, M., S. Bhattacharjee, G. K. Das, and M. Mitra, "Dual-band dual-polarized compact planar monopole antenna for wide axial ratio bandwidth application," *International Journal of RF and Microwave Computer-Aided Engineering*, e22152, 2020.
17. Xu, R., J. Li, Y.-X. Qi, G. W. Yang, and J.-J. Yang, "A design of triple wideband triple-sense circularly polarized square slot antenna," *IEEE Antennas and Wireless Propagation Letters*, Vol. 16, 1763–1766, 2017.
18. Behera, H. K. and L. P. Mishra, "Comparison of different shapes for micro-strip antenna design. Advances in intelligent computing and communication," *Lecture Notes in Networks and Systems*, Vol. 430, Springer, Singapore, 2022.